PROCEEDINGS OF THE ROYAL SOCIETY A

Proc. R. Soc. A (2006) **462**, 839–854
doi:10.1098/rspa.2005.1598
Published online 10 January 2006

Analytical models for bistable cylindrical shells

By S. D. Guest* and S. Pellegrino

Department of Engineering, University of Cambridge, Trumpington Street, Cambridge CB2 1PZ, UK

Thin cylindrical shell structures can show interesting bistable behaviour. If made unstressed from isotropic materials they are only stable in the initial configuration, but if made from fibre-reinforced composites they may also have a second, stable configuration. If the layup of the composite is antisymmetric, this alternative stable configuration forms a tight coil; if the layup is symmetric the alternative stable configuration is helical. A simple two-parameter model for these structure is presented that is able to distinguish between these different behaviours.

Keywords: shell structure; bistable; composite materials

1. Introduction and background

This paper presents simple analytical models for a class of thin shell structures that have the interesting and useful property of bistability. These structures have the same initial geometry as a standard, steel tape measure: they are straight in the longitudinal direction and have a curved cross-section. However, unlike a tape measure, these structures are stable both in the unstressed, straight configuration and also in a coiled configuration. The bistability in the structures that we consider is engendered by specifying certain relative bending stiffnesses of the shell using, for instance, fibre-reinforced composites. An alternative technique for making these structures bistable, by setting up an initial state of self-stress in the shell, is described by Kebadze *et al.* (2004).

Recent work on bistable cylindrical shells (Iqbal & Pellegrino 2000; Iqbal *et al.* 2000; Galletly & Guest 2004*a*,*b*) has generated a number of analytical and computational models that capture various aspects of their behaviour, with varying degrees of detail and accuracy. However, none of these models is sufficiently compact to be able to capture all of the key effects in a set of analytical expressions. Hence, starting from the observation that many features of interest can be captured by a model that considers only uniform, inextensionally deformed configurations of the shell, a new model is presented that expresses the equilibrium and stability conditions of the shell in terms of only two parameters.

The paper is laid out as follows. Section 2 introduces the geometry and material properties of the structures to be studied. Section 3 outlines a previously

* Author for correspondence (sdg@eng.cam.ac.uk).

Received 4 May 2005
Accepted 18 October 2005

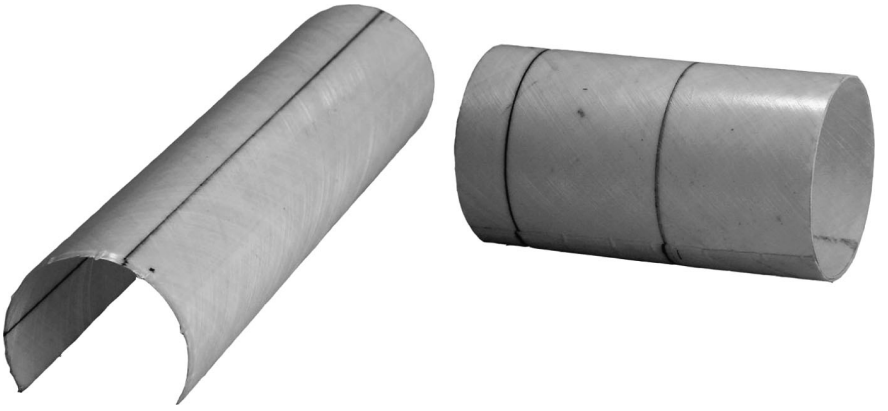

Figure 1. A bistable shell shown in its initial and coiled configuration. Two lines are marked on the shell: they are straight initially, and form circles in the coiled configuration.

developed analytical model for bistable shells which allows both extension and bending to take place in the shell. On the basis of results obtained from this model, it is then argued that an inextensional model that includes twisting will provide a more complete description of the required behaviour, but still in terms of only two geometric parameters. Section 4 presents this new model, and derives analytically the equations that need to be solved to find all of the equilibrium configurations of a cylindrical shell. An analytical criterion for stability is also derived. Four examples are then presented and discussed in detail. Section 5 derives a simple stability criterion for shells where bending and twisting are decoupled. Section 6 discusses an extension of the formulation in §4 that allows uniform mid-surface strains of the shell. Sections 7 and 8 conclude the paper.

2. Bistable shells

Figure 1 shows a bistable cylindrical shell. It is made from a fibre-reinforced composite, with the fibres arranged antisymmetrically with respect to the mid-plane; this results in a structure that is stable in the two configurations shown. Note that in the second configuration the structure is coiled, with a longitudinal curvature that is in the same sense as the transverse curvature of the first configuration, i.e. the centres of curvature in the two stable states are on the same side of the structure.

It is rather unusual for a composite structure to be made from an antisymmetric layup, but here this particular arrangement is chosen in order to achieve a compact coiled configuration. If a model is instead made from a symmetric layup, the second configuration would actually be twisted.

In this paper, it will be assumed that the structure is formed initially stress-free in the extended state, shown in figure 2. In this initial configuration, it is straight, has uniform cross-section and can be treated as linear-elastic and infinitely long in the longitudinal x-direction. It has a radius of curvature of R in the transverse, y-direction, and subtends an angle β.

The models described here will assume that the deformation of the structure is uniform in the longitudinal direction, and, hence, make no attempt to model the

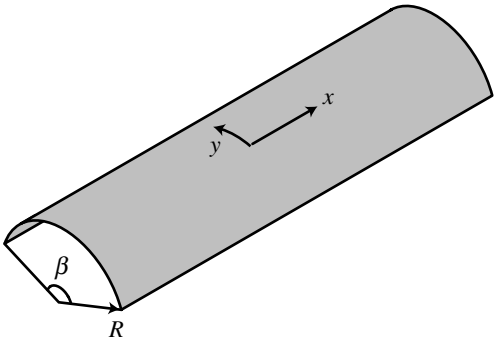

Figure 2. The initial, stress-free configuration for a bistable shell.

actual transformation from the extended to the coiled configuration, which in reality takes place by a short transition zone moving along the structure. Therefore, the models are trying to capture only the two extreme configurations.

The bending and stretching properties of the shell will be described in terms of classical thin-plate lamination theory (Jones 1999). Hence, the coupled stress–strain and moment–curvature relationships take the form of the standard ***ABD*** matrix relating the generalized strain vector $\Delta[\varepsilon_x, \varepsilon_y, \gamma_{xy}, \kappa_x, \kappa_y, \kappa_{xy}]^{\mathrm{T}}$ to the work-conjugate generalized stress vector $[N_x, N_y, N_{xy}, M_x, M_y, M_{xy}]^{\mathrm{T}}$

$$\begin{bmatrix} N_x \\ N_y \\ N_{xy} \\ - \\ M_x \\ M_y \\ M_{xy} \end{bmatrix} = \left[\begin{array}{ccc|ccc} A_{11} & A_{12} & A_{16} & B_{11} & B_{12} & B_{16} \\ A_{12} & A_{22} & A_{26} & B_{12} & B_{22} & B_{26} \\ A_{16} & A_{26} & A_{66} & B_{16} & B_{26} & B_{66} \\ - & - & - & - & - & - \\ \hline B_{11} & B_{12} & B_{16} & D_{11} & D_{12} & D_{16} \\ B_{12} & B_{22} & B_{26} & D_{12} & D_{22} & D_{26} \\ B_{16} & B_{26} & B_{66} & D_{16} & D_{26} & D_{66} \end{array}\right] \Delta \begin{bmatrix} \epsilon_x \\ \epsilon_y \\ \gamma_{xy} \\ - \\ \kappa_x \\ \kappa_y \\ \kappa_{xy} \end{bmatrix}. \tag{2.1}$$

Here, $\Delta\epsilon_x$, $\Delta\epsilon_y$, $\Delta\gamma_{xy}$ are the mid-plane strains associated with moving from the original configuration to any configuration of interest, and $\Delta\kappa_x$, $\Delta\kappa_y$, $\Delta\kappa_{xy}$ are the corresponding mid-surface curvatures. (Note that (2.1) assumes that the twisting curvature is defined as $\kappa_{xy} = -2\partial^2 w/\partial x\,\partial y$, where w is the displacement of the surface in the out-of-plane direction. The plate and shell theory literature conventionally defines κ_{xy} to be half this value; the connection is made in, e.g., Mansfield (1989), p. 25).

Four specific examples will be presented later on: one is an isotropic shell (0.125 mm thick steel); the other three are orthotropic structures, with various antisymmetric and symmetric layups, each made of five, 0.21 mm thick layers of uniaxial glass fibres in a polypropylene matrix. The material properties are listed in table 1, and table 2 shows the ***ABD*** matrices for the four examples.

Table 1. Material properties (directions 1, 2 are along and perpendicular to fibres).

steel	E	207 GPa
	ν	0.3
glass–polypropylene	E_{11}	27.6 GPa
	E_{22}	2.60 GPa
	G	0.964 GPa
	ν_{12}	0.305

Table 2. **ABD** matrices for four examples (all units are in GN, mm).

isotropic shell	$\left[\begin{array}{ccc\|ccc} 28.43 & 8.53 & 0 & 0 & 0 & 0 \\ 8.53 & 28.43 & 0 & 0 & 0 & 0 \\ 0 & 0 & 9.95 & 0 & 0 & 0 \\ \hline 0 & 0 & 0 & 0.0370 & 0.0111 & 0 \\ 0 & 0 & 0 & 0.0111 & 0.0370 & 0 \\ 0 & 0 & 0 & 0 & 0 & 0.0130 \end{array}\right]$
antisymmetric 45° layup, [+45°, −45°, 0°, +45°, −45°]	$\left[\begin{array}{ccc\|ccc} 13.32 & 6.06 & 0 & 0 & 0 & 0.550 \\ 6.06 & 8.05 & 0 & 0 & 0 & 0.550 \\ 0 & 0 & 6.23 & 0.550 & 0.550 & 0 \\ \hline 0 & 0 & 0.550 & 0.868 & 0.665 & 0 \\ 0 & 0 & 0.550 & 0.665 & 0.848 & 0 \\ 0.550 & 0.550 & 0 & 0 & 0 & 0.681 \end{array}\right]$
symmetric 45° layup, [+45°, −45°, 0°, −45°, +45°]	$\left[\begin{array}{ccc\|ccc} 13.32 & 6.06 & 0 & 0 & 0 & 0 \\ 6.06 & 8.05 & 0 & 0 & 0 & 0 \\ 0 & 0 & 6.23 & 0 & 0 & 0 \\ \hline 0 & 0 & 0 & 0.868 & 0.665 & 0.345 \\ 0 & 0 & 0 & 0.665 & 0.848 & 0.345 \\ 0 & 0 & 0 & 0.345 & 0.345 & 0.681 \end{array}\right]$
symmetric 40° layup, [+40°, −40°, 0°, −40°, +40°]	$\left[\begin{array}{ccc\|ccc} 15.30 & 5.90 & 0 & 0 & 0 & 0 \\ 5.90 & 6.38 & 0 & 0 & 0 & 0 \\ 0 & 0 & 6.07 & 0 & 0 & 0 \\ \hline 0 & 0 & 0 & 1.092 & 0.647 & 0.398 \\ 0 & 0 & 0 & 0.647 & 0.660 & 0.281 \\ 0 & 0 & 0 & 0.398 & 0.281 & 0.663 \end{array}\right]$

3. Extensional bending model

A simple extensional bending model for bistable shells was first presented by Iqbal & Pellegrino (2000). This model considers a general configuration of the shell with uniform longitudinal curvature, κ_x and transverse curvature, κ_y, as shown in figure 3. No twisting is allowed, i.e. $\kappa_{xy}=0$ everywhere, and stretching–bending coupling will be ignored when constructing the strain energy expression, i.e. it will be assumed that $B=0$.

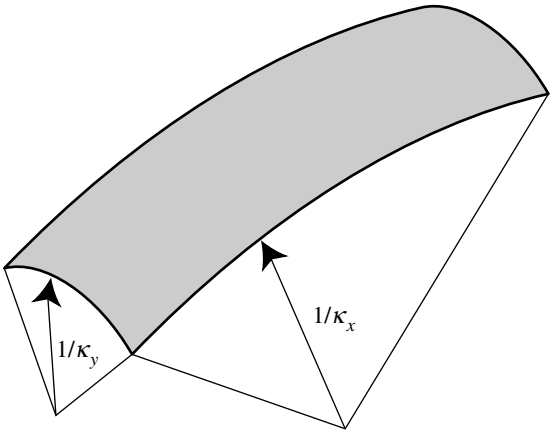

Figure 3. A shell with uniform curvatures κ_x and κ_y.

Generally, in these configurations, the shell has both bending and stretching strain energy. These energy terms have the following expressions, per unit area (Mansfield 1989):

$$U_{\mathrm{b}} = \frac{1}{2}\boldsymbol{k}^{\mathrm{T}}\boldsymbol{D}\boldsymbol{k}, \tag{3.1}$$

$$U_{\mathrm{s}} = \frac{1}{2}\boldsymbol{\epsilon}^{\mathrm{T}}\boldsymbol{A}\boldsymbol{\epsilon}, \tag{3.2}$$

where the bending stiffnesses of the shell are defined by the $\boldsymbol{D}$-matrix portion of the $\boldsymbol{ABD}$ matrix, which relates moments per unit length, $\boldsymbol{m} = [m_x, m_y, m_{xy}]^{\mathrm{T}}$, and change of mid-surface curvatures, $\boldsymbol{k} = \Delta[\kappa_x, \kappa_y, \kappa_{xy}]^{\mathrm{T}}$,

$$\boldsymbol{m} = \boldsymbol{D}\boldsymbol{k} \tag{3.3}$$

and the stretching stiffnesses of the shell are defined by the $\boldsymbol{A}$-matrix portion of $\boldsymbol{ABD}$ which relates in-plane forces per unit length, $\boldsymbol{f} = [f_x, f_y, f_{xy}]^{\mathrm{T}}$, and mid-surface strains, $\boldsymbol{\epsilon} = \Delta[\epsilon_x, \epsilon_y, \gamma_{xy}]^{\mathrm{T}}$,

$$\boldsymbol{f} = \boldsymbol{A}\boldsymbol{\epsilon}. \tag{3.4}$$

Iqbal & Pellegrino (2000) integrated (3.1) and (3.2) over the cross-section of the shell and obtained the following expression for the average strain energy per unit area,

$$\begin{aligned} U = {} & \frac{1}{\beta R}\,\frac{A_{11}}{2}\left[\frac{\beta R}{2}\,\frac{\kappa_x^2}{\kappa_y^2} + \frac{\sin(\beta R\kappa_y)}{2}\,\frac{\kappa_x^2}{\kappa_y^3} - \frac{4\sin^2(\beta R\kappa_y/2)}{\beta R}\,\frac{\kappa_x^2}{\kappa_y^4}\right] \\ & + \frac{1}{2}\left[D_{11}\kappa_x^2 + 2D_{12}\kappa_x\left(\kappa_y - \frac{1}{R}\right) + D_{22}\left(\kappa_y - \frac{1}{R}\right)^2\right]. \end{aligned} \tag{3.5}$$

The terms in this equation can be written in non-dimensional form (written with a hat) in terms of the bending stiffness in the x-direction, D_{11}, and the initial

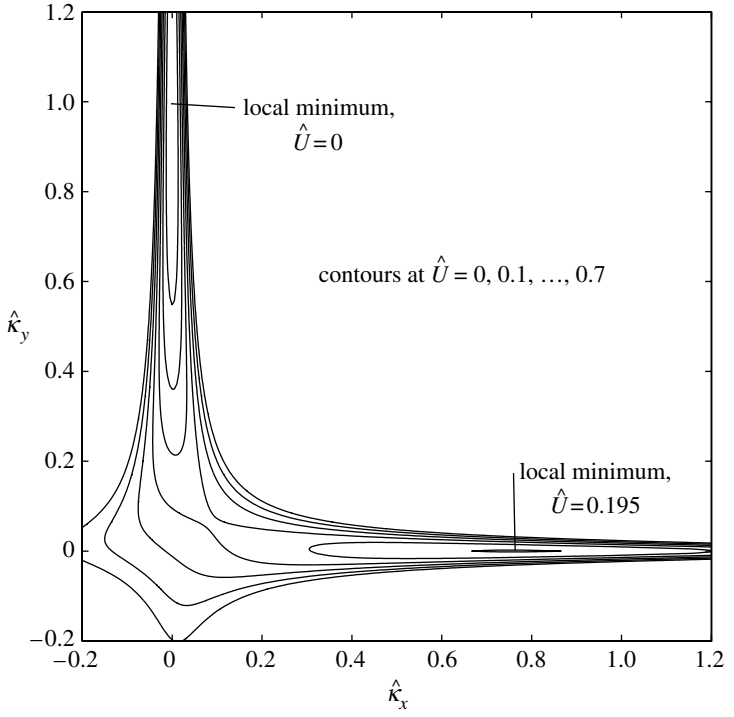

Figure 4. The non-dimensional strain energy stored by the antisymmetric 45° layup for $\beta=\pi$.

radius of curvature, R, as

$$\hat{U}=\frac{UR^2}{D_{11}},\quad \hat{A}_{11}=\frac{A_{11}R^2}{D_{11}},\quad \hat{D}_{12}=\frac{D_{12}}{D_{11}},\quad \hat{D}_{22}=\frac{D_{22}}{D_{11}},\quad \hat{\kappa}_y=R\kappa_y,\quad \hat{\kappa}_x=R\kappa_x,$$

giving an equivalent expression for energy

$$\begin{aligned}\hat{U}=\frac{\hat{A}_{11}}{4}\frac{\hat{\kappa}_x^2}{\hat{\kappa}_y^2}\left[1+\frac{\sin(\beta\hat{\kappa}_y)}{\hat{\kappa}_y}-\frac{8\sin^2(\beta\hat{\kappa}_y/2)}{\hat{\kappa}_y^2}\right]\\ +\frac{1}{2}\left[\hat{\kappa}_x^2+2\hat{D}_{12}\hat{\kappa}_x(\hat{\kappa}_y-1)+\hat{D}_{22}(\hat{\kappa}_y-1)^2\right].\end{aligned}\tag{3.6}$$

Figure 4 shows a contour plot of the values given by (3.6) for varying $\hat{\kappa}_x$ and $\hat{\kappa}_y$. The shell stiffness parameters chosen are those for the antisymmetric 45° layup (given in table 2), and the angle subtended by the cross-section is $\beta=\pi$.

There are a number of interesting points about the plot in figure 4. The first is that it clearly shows the existence of two energy minima, one in the original configuration, and another in the coiled configuration. Another observation is that there is a severe energy penalty associated with stretching, rather than bending, the mid-surface and hence the behaviour of interest is concentrated in, or near the regions of the plot, where $\hat{\kappa}_x\hat{\kappa}_y\approx 0$.

This extensional model may be misleading for more general material properties, however, where the assumption that the shell does not twist cannot

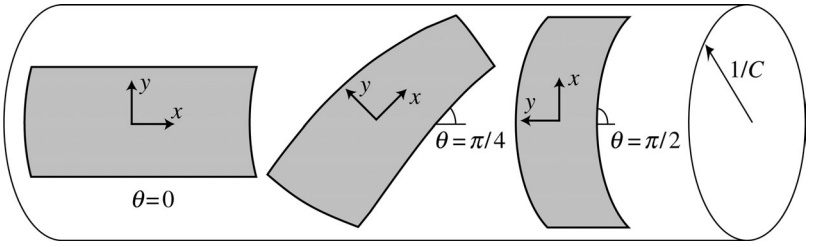

Figure 5. The coordinate system used in §4. Three shells are shown on an underlying cylinder of radius $1/C$.

be justified. For example, for the *symmetric* 45° layup, exactly the same plot shown in figure 4 would be obtained, but here the $\boldsymbol{ABD}$ matrix shows bend/twist coupling and twisted configurations of the shell should not be excluded. Further, *stability* in torsion cannot be examined, which proves to be important for isotropic shells.

Galletly & Guest (2004*a*) have extended this model to include twist, and thus allow a distinction to be made between symmetric and antisymmetric layups. This extended model also captures the unstable nature of the second equilibrium configuration for unstressed, isotropic shells. However, the model is also fairly complex, partly because it requires a third parameter to define the twist.

The clue to developing a simpler model is contained in the plot in figure 4. The earlier observation that the interesting behaviour is concentrated, where $\hat{\kappa}_x\hat{\kappa}_y \approx 0$ suggests setting up a model that assumes all deformations to be inextensional.

4. Inextensional model

This section develops a model that simplifies the analysis of the shells by assuming that the mid-surface does not stretch. It will examine all possible inextensional deformations that are everywhere uniform, and look for energy minima in order to find stable configurations.

The initial configuration has principal curvatures $\kappa_1 = 1/R$ and $\kappa_2 = 0$, and so for inextensional deformation the Gaussian curvature $(=\kappa_1 \times \kappa_2)$ must remain zero. This implies that all possible configurations must be *developable* (Calladine 1983). In this section we shall assume that the deformation of the shell is everywhere uniform: this implies that for every possible configuration of the shell there must be an underlying cylinder about which the shell is wrapped. Thus, every possible configuration of the shell can be defined by two variables, one defining the radius of this underlying cylinder, and the other defining the orientation of the shell relative to the cylinder.

Figure 5 shows the coordinates that will be used in this section. The angle of the shell relative to the cylinder, θ, is defined so that $\theta = 0$ when the shell is parallel with the axis of the cylinder. The principal curvature of the cylinder is C and so the radius of the cylinder is $1/C$.

For any C and θ, the curvature of the shell in the x–y coordinate system shown in figure 2 can be found using a Mohr's circle (Calladine 1983), as shown in figure 6. In the initial configuration, $\kappa_x = 0$, $\kappa_y = 1/R$, $\kappa_{xy} = 0$. In the final configuration, $\kappa_x = (C/2)(1 - \cos 2\theta)$, $\kappa_y = (C/2)(1 + \cos 2\theta)$, $\kappa_{xy} = C \sin 2\theta$.

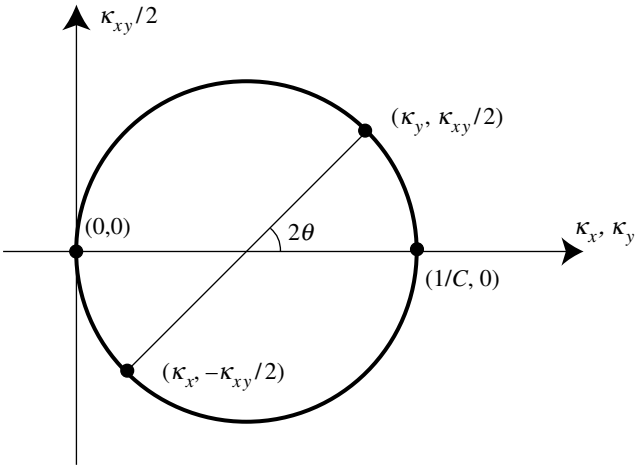

Figure 6. Mohr's circle of curvature. The vertical axis is $\kappa_{xy}/2$ rather than κ_{xy}, as we are using the lamination theory definition of twist.

Thus, the changes in curvature are given by

$$\Delta\begin{bmatrix}\kappa_x\\ \kappa_y\\ \kappa_{xy}\end{bmatrix}=\frac{C}{2}\begin{bmatrix}1-\cos 2\theta\\ \cos 2\theta+1\\ 2\sin 2\theta\end{bmatrix}-\begin{bmatrix}0\\ \dfrac{1}{R}\\ 0\end{bmatrix}. \tag{4.1}$$

The bending strain energy per unit area, given by (3.1), can be written using non-dimensional variables (again, written with a hat)

$$\hat{U}=\frac{UR^2}{D_{11}},\quad \hat{\boldsymbol{D}}=\frac{\boldsymbol{D}}{D_{11}},\quad \hat{\boldsymbol{k}}=R\boldsymbol{k}=\frac{CR}{2}\begin{bmatrix}1-\cos 2\theta\\ \cos 2\theta+1-\dfrac{2}{RC}\\ 2\sin 2\theta\end{bmatrix},\quad \hat{C}=CR,$$

as

$$\hat{U}=\frac{1}{2}\hat{\boldsymbol{k}}^{\mathrm{T}}\hat{\boldsymbol{D}}\hat{\boldsymbol{k}}. \tag{4.2}$$

To find stable equilibria, we look to minimize $\hat{U}$ subject to the inextensional constraint given in (4.1); i.e. we are looking for minima with respect to the two variables θ and $\hat{C}$. We can explore variations in $\hat{U}$ locally by considering the change in energy, $\delta\hat{U}$, for small variations in θ and $\hat{C}$, $\delta\theta$ and $\delta\hat{C}$, using the Taylor's series expansion (e.g. Riley *et al.* 1997) given by

$$\delta\hat{U}=\frac{\partial\hat{U}}{\partial\theta}\delta\theta+\frac{\partial\hat{U}}{\partial\hat{C}}\delta\hat{C}+\frac{1}{2}[\,\delta\theta\quad\delta\hat{C}\,]\begin{bmatrix}\partial^2\hat{U}/\partial\theta^2 & \partial^2\hat{U}/\partial\theta\,\partial\hat{C}\\ \partial^2\hat{U}/\partial\theta\,\partial\hat{C} & \partial^2\hat{U}/\partial\hat{C}^2\end{bmatrix}\begin{bmatrix}\delta\theta\\ \delta\hat{C}\end{bmatrix}+\cdots. \tag{4.3}$$

To find equilibrium configurations of the structure, we look for points where locally the energy has zero slope for changes in θ and $\hat{C}$, and hence the first two

terms in (4.3) are zero. Differentiating (4.2) gives

$$\frac{\partial \hat{U}}{\partial \theta} = \hat{\boldsymbol{k}}^{\mathrm{T}} \hat{\boldsymbol{D}} \frac{\partial \hat{\boldsymbol{k}}}{\partial \theta} = 0, \quad \frac{\partial \hat{U}}{\partial \hat{C}} = \hat{\boldsymbol{k}}^{\mathrm{T}} \hat{\boldsymbol{D}} \frac{\partial \hat{\boldsymbol{k}}}{\partial \hat{C}} = 0, \tag{4.4}$$

where from (4.1)

$$\frac{\partial \hat{\boldsymbol{k}}}{\partial \theta} = \frac{\hat{C}}{2} \begin{bmatrix} 2\sin 2\theta \\ -2\sin 2\theta \\ 4\cos 2\theta \end{bmatrix}, \quad \frac{\partial \hat{\boldsymbol{k}}}{\partial \hat{C}} = \frac{1}{2} \begin{bmatrix} 1-\cos 2\theta \\ \cos 2\theta + 1 \\ 2\sin 2\theta \end{bmatrix}.$$

Solving (4.4) will determine pairs of θ and $\hat{C}$ that define *equilibrium configurations*, but to check whether these are *stable* equilibria, we need to check whether they correspond to local minima. This we do by considering the next term in the Taylor series expansion (4.3), and check that

$$\hat{K} = \begin{bmatrix} \partial^2 \hat{U}/\partial \theta^2 & \partial^2 \hat{U}/\partial \theta \, \partial \hat{C} \\ \partial^2 \hat{U}/\partial \theta \, \partial \hat{C} & \partial^2 \hat{U}/\partial \hat{C}^2 \end{bmatrix}, \tag{4.5}$$

is positive definite. Note that $\hat{K}$ is a stiffness matrix for the structure.

The positive definiteness of (4.5) can be analysed by checking that

$$\frac{\partial^2 \hat{U}}{\partial \theta^2} > 0, \quad \frac{\partial^2 \hat{U}}{\partial \hat{C}^2} > 0 \quad \text{and} \quad \left(\frac{\partial^2 \hat{U}}{\partial \hat{C}^2}\right)\left(\frac{\partial^2 \hat{U}}{\partial \theta^2}\right) > \left(\frac{\partial^2 \hat{U}}{\partial \theta \, \partial \hat{C}}\right)^2. \tag{4.6}$$

The terms in these inequalities are given by

$$\frac{\partial^2 \hat{U}}{\partial \hat{C}^2} = \frac{\partial \hat{\boldsymbol{k}}^{\mathrm{T}}}{\partial \hat{C}} \hat{\boldsymbol{D}} \frac{\partial \hat{\boldsymbol{k}}}{\partial \hat{C}}, \tag{4.7}$$

as $\partial^2 \hat{\boldsymbol{k}}/\partial \hat{C}^2 = \boldsymbol{0}$, and

$$\frac{\partial^2 \hat{U}}{\partial \theta^2} = \frac{\partial \hat{\boldsymbol{k}}^{\mathrm{T}}}{\partial \theta} \hat{\boldsymbol{D}} \frac{\partial \hat{\boldsymbol{k}}}{\partial \theta} + \hat{\boldsymbol{k}}^{\mathrm{T}} \hat{\boldsymbol{D}} \frac{\partial^2 \hat{\boldsymbol{k}}}{\partial \theta^2}, \tag{4.8}$$

where

$$\frac{\partial^2 \hat{\boldsymbol{k}}}{\partial \theta^2} = \frac{\hat{C}}{2} \begin{bmatrix} 4\cos 2\theta \\ -4\cos 2\theta \\ -8\sin 2\theta \end{bmatrix},$$

and

$$\frac{\partial^2 \hat{U}}{\partial \theta \, \partial \hat{C}} = \frac{\partial \hat{\boldsymbol{k}}^{\mathrm{T}}}{\partial \hat{C}} \hat{\boldsymbol{D}} \frac{\partial \hat{\boldsymbol{k}}}{\partial \theta} + \hat{\boldsymbol{k}}^{\mathrm{T}} \hat{\boldsymbol{D}} \frac{\partial^2 \hat{\boldsymbol{k}}}{\partial \theta \, \partial \hat{C}}, \tag{4.9}$$

where

$$\frac{\partial^2 \hat{\boldsymbol{k}}}{\partial \theta \, \partial \hat{C}} = \frac{1}{2} \begin{bmatrix} 2\sin 2\theta \\ -2\sin 2\theta \\ -4\cos 2\theta \end{bmatrix}.$$

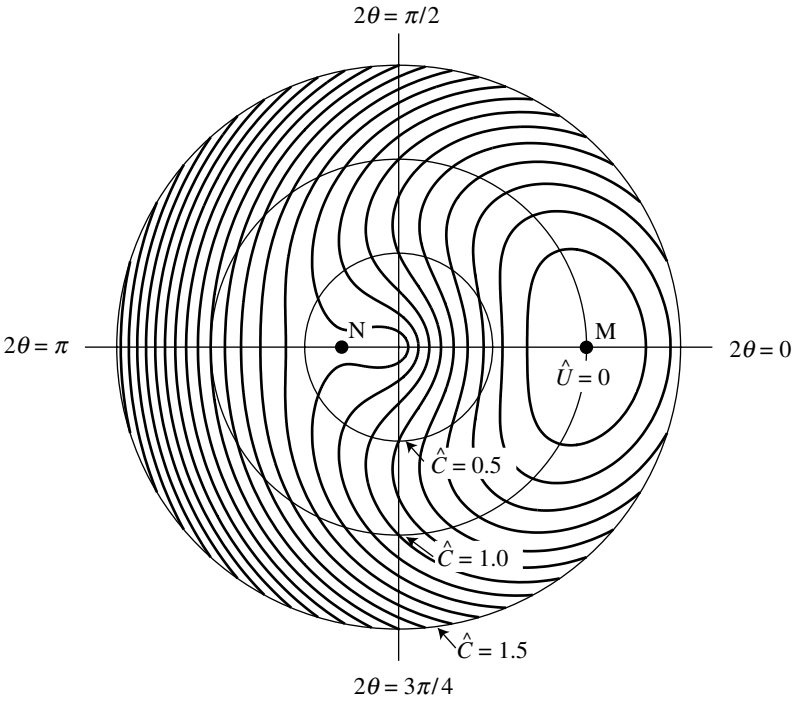

Figure 7. Polar plot of non-dimensional energy $\hat{U}$ plotted as a function of $\hat{C}$ and θ for the isotropic shell example. Contours are plotted at $\hat{U} = 0.05, 0.1, 0.15, \ldots$. The two equilibrium points are labelled M and N.

The energy as a function of $\hat{C}$ and θ, equilibrium points, and the stability of these equilibria, will be considered for the four examples described in §2. Energy will be plotted in each case on a polar plot for $0 \leq 2\theta < 2\pi$, which covers the full range of possible positions, and for $0 \leq \hat{C} \leq 1.5$, which covers all of the interesting behaviour for these examples.

(*a*) *Isotropic example*

For the isotropic shell described in table 2, the non-dimensional $\boldsymbol{D}$-matrix is given by

$$\hat{\boldsymbol{D}} = \begin{bmatrix} 1 & 0.3 & 0 \\ 0.3 & 1 & 0 \\ 0 & 0 & 0.35 \end{bmatrix}. \tag{4.10}$$

(In conventional plate and shell theory, the (3,3) term of this matrix is given by $1-\nu$, but here it is $(1-\nu)/2$, as we are using the lamination theory definition of twist.)

Figure 7 shows the non-dimensional energy, calculated from (4.2) for this shell; there are two equilibrium positions, that have been labelled M and N. The first equilibrium, M, is the original configuration, $\theta = 0$, $\hat{C} = 1$, where clearly there is an energy minimum. The second equilibrium, N, is at $\theta = \pi/2$, $\hat{C} = 0.3 = \nu$; substituting these values into (4.4) will verify that this satisfies $\partial\hat{U}/\partial\theta = \partial\hat{U}/\partial\hat{C} = 0$.

Although there is a second equilibrium point N, it is clear from the plot that this point is a saddle point in the energy. This can be verified from (4.7) and (4.8), which gives $\partial^2\hat{U}/\partial\hat{C}^2 = 1$, $\partial^2\hat{U}/\partial\theta^2 = -0.42$. Hence, this second equilibrium point is not stable. This result can be verified by taking a length of steel tape measure and attempting to coil it to a radius of about 1/3 the radius of the cross-section: an unstable twisting mode can be observed.

As for all the energy plots in this section, there is an apparent maximum at $\hat{C} = 0$. However, this is an artefact of the way the plots are drawn, and is not an equilibrium position. It can be readily verified that $\partial\hat{U}/\partial\hat{C} \neq 0$ at $\hat{C} = 0$.

(*b*) *Antisymmetric* 45° *composite example*

For the antisymmetric composite shell described in table 2, the non-dimensional $\boldsymbol{D}$-matrix is given by

$$\hat{\boldsymbol{D}} = \begin{bmatrix} 1 & 0.766 & 0 \\ 0.766 & 0.977 & 0 \\ 0 & 0 & 0.785 \end{bmatrix}. \tag{4.11}$$

It is interesting to compare this matrix with that for the isotropic case. Because of the antisymmetry, there is again no coupling between bending and twisting, and the basic form of the matrix is the same, with $\hat{D}_{16} = \hat{D}_{26} = 0$. The key differences, however, are the approximate doubling of the relative coupling between bending in the x- and y-directions, $\hat{D}_{12}$, and the approximate doubling of the relative twisting stiffness, $\hat{D}_{66}$.

Figure 8 shows the non-dimensional energy, calculated from (4.2), for the antisymmetric composite shell. There are now four equilibrium positions, labelled M, N, P and Q. The first equilibrium, M, is the original configuration, $\theta = 0$, $\hat{C} = 1$, where clearly there is an energy minimum. The second equilibrium, N, is at $\theta = \pi/2$, $\hat{C} = \hat{D}_{12} = 0.77$; substituting into (4.4) will verify that this satisfies the equilibrium conditions $\partial\hat{U}/\partial\theta = \partial\hat{U}/\partial\hat{C} = 0$.

The form of the contour plot shows clearly that N is a minimum, and this can be verified by checking (4.7)–(4.9), which give $\partial^2\hat{U}/\partial\hat{C}^2 = 1$, $\partial^2\hat{U}/\partial\theta^2 = 1.24$, $\partial^2\hat{U}/\partial\theta\,\partial\hat{C} = 0$. The third and fourth equilibrium positions, P and Q, are at $\theta = \pm 0.30\pi$, $\hat{C} = 0.52$. These are clearly saddle points, and will not be explored further.

(*c*) *Symmetric* 45° *composite example*

For the symmetric 45° composite shell described in table 2, the non-dimensional $\boldsymbol{D}$-matrix is given by

$$\hat{\boldsymbol{D}} = \begin{bmatrix} 1 & 0.766 & 0.397 \\ 0.766 & 0.977 & 0.397 \\ 0.397 & 0.397 & 0.785 \end{bmatrix}. \tag{4.12}$$

Figure 9 shows the non-dimensional energy, calculated using (4.2) for this case. An interesting observation is that, because of the coupling between bending and twisting, the symmetry of the plot about the lines $\theta = 0$, $\pi/2$ has been lost.

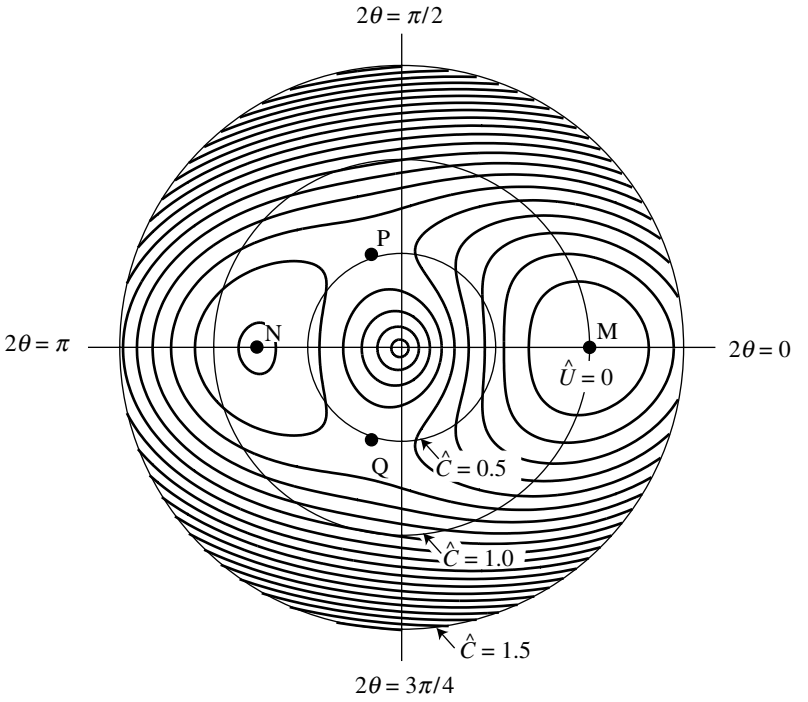

Figure 8. Polar plot of non-dimensional energy $\hat{U}$ versus $\hat{C}$ and θ for the antisymmetric composite shell example. Contours are plotted at $\hat{U} = 0.05, 0.1, 0.15, \ldots$. The four equilibrium points are labelled M, N, P and Q.

There are four equilibrium positions shown in figure 9, labelled M, N, P and Q. The first is the original configuration, $\theta = 0$, $\hat{C} = 1$, where clearly there is an energy minimum. The other obvious equilibrium is at Q, where $\theta = 0.72\pi$, $\hat{C} = 0.54$; substituting into (4.4) will verify that this satisfies $\partial\hat{U}/\partial\theta = \partial\hat{U}/\partial\hat{C} = 0$. However, at this position, from (4.7) and (4.8), $\partial^2\hat{U}/\partial\hat{C}^2 = 0.86$ and $\partial^2\hat{U}/\partial\theta^2 = -1.15$, which shows that this equilibrium point is a saddle point, and is not stable.

Careful study of the equilibrium equations shows that there are in fact two other equilibria that are almost superimposed, N at $\theta = 0.41\pi$, $\hat{C} = 0.62$, and P at $\theta = 0.40\pi$, $\hat{C} = 0.60$. N is a second energy minimum and P is a second saddle point in the energy. Thus the shell is bistable, but the stability of N is clearly marginal. The region around N and P is shown more clearly for the symmetric 40° composite shell, in the next example.

(*d*) *Symmetric* 40° *composite example*

For the symmetric 40° composite shell described in table 2, the non-dimensional $\boldsymbol{D}$-matrix is given by

$$\hat{\boldsymbol{D}} = \begin{bmatrix} 1 & 0.593 & 0.364 \\ 0.593 & 0.604 & 0.257 \\ 0.364 & 0.257 & 0.607 \end{bmatrix}. \tag{4.13}$$

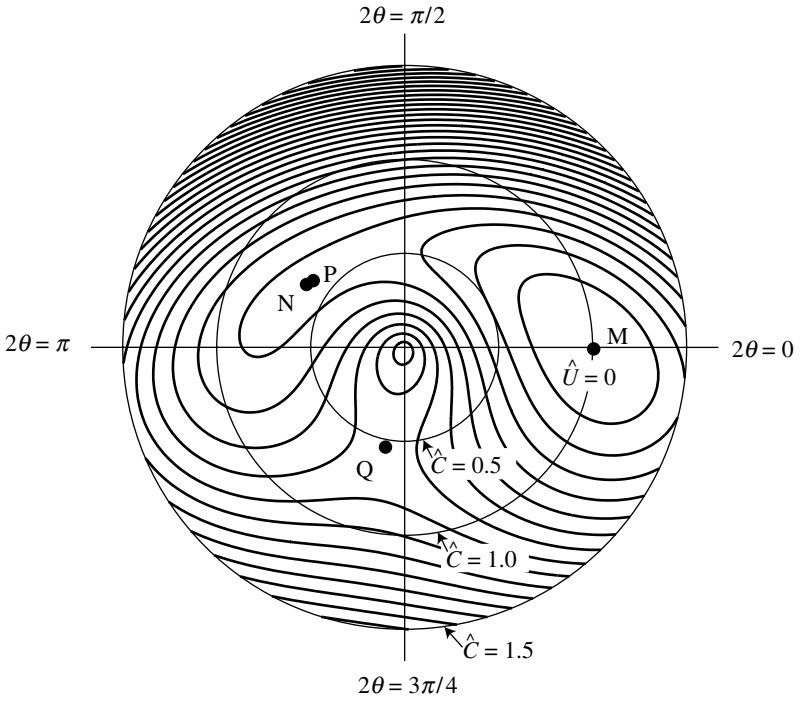

Figure 9. Polar plot of non-dimensional energy $\hat{U}$ versus $\hat{C}$ and θ for the symmetric composite shell example. Contours are plotted at $\hat{U} = 0.05, 0.1, 0.15, \ldots$. The four equilibrium points are labelled M, N, P and Q.

Figure 10 shows the non-dimensional energy, calculated from (4.2) for this case. The basic structure of the plot is very similar to the 45° symmetric case; again there are four equilibrium positions, labelled M, N, P and Q, but now N and P are shown distinctly.

The equilibrium point M is the original configuration, a minimum at $\theta = 0$, $\hat{C} = 1$, and there is a saddle point Q, now at $\theta = 0.74\pi$, $\hat{C} = 0.50$. The second minimum, N, is at $\theta = 0.44\pi$, $\hat{C} = 0.52$. Substituting into (4.7)–(4.9) gives $\partial^2\hat{U}/\partial\hat{C}^2 = 1.31$, $\partial^2\hat{U}/\partial\theta^2 = 0.29$, $\partial^2\hat{U}/\partial\theta\,\partial\hat{C} = -0.49$, confirming that this is indeed a minimum, and that the structure is bistable. The second saddle-point, P, is at $\theta = 0.38\pi$, $\hat{C} = 0.46$. Substituting into (4.7)–(4.9) gives $\partial^2\hat{U}/\partial\hat{C}^2 = 1.67$, $\partial^2\hat{U}/\partial\theta^2 = 0.0032$, $\partial^2\hat{U}/\partial\theta\partial\hat{C} = -0.38$, confirming that this is a saddle-point.

5. Stability criterion for shells with no coupling between bending and twisting

The results from §§4*a*,*b* can be generalized to give a stability criterion for any shell, where there is no coupling between bending and twisting ($D_{16} = D_{26} = 0$). In this case, there will always be a solution of the equilibrium equations (4.4) at $\theta = \pi/2$, $\hat{C} = \hat{D}_{12}$, corresponding to a second equilibrium position in addition to

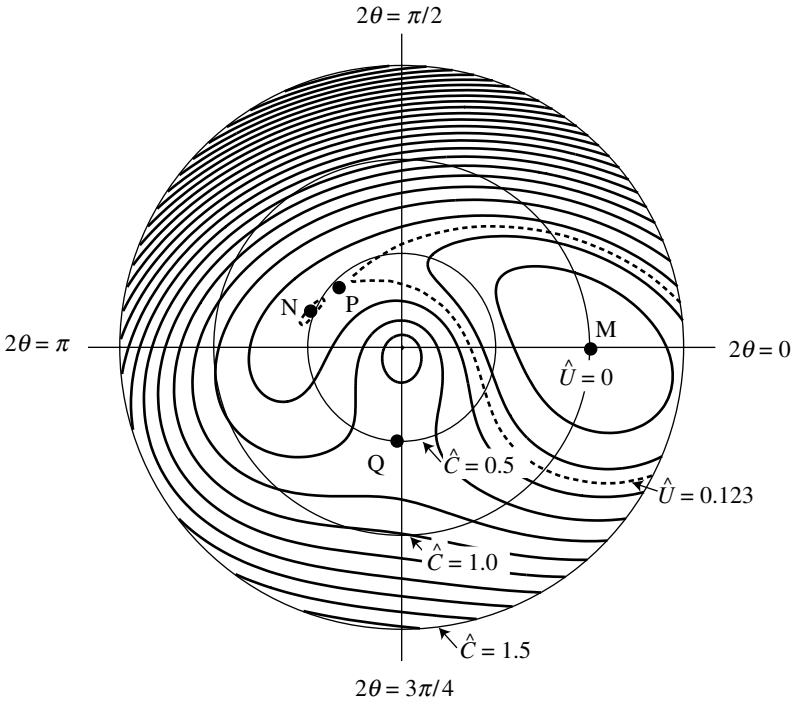

Figure 10. Polar plot of non-dimensional energy $\hat{U}$ versus $\hat{C}$ and θ for the 40° symmetric composite shell example. Contours are plotted at $\hat{U} = 0.05, 0.1, 0.15, \ldots$. The four equilibrium points are labelled M, N, P and Q. The additional contour $\hat{U} = 0.123$ has been plotted as a dashed line to show more clearly the nature of the equilibria at N and P.

the initial point at

$$\hat{\boldsymbol{k}} = \begin{bmatrix} \hat{D}_{12} \\ -1 \\ 0 \end{bmatrix},$$

where

$$\frac{\partial \hat{\boldsymbol{k}}}{\partial \theta} = \hat{D}_{12} \begin{bmatrix} 0 \\ 0 \\ -2 \end{bmatrix}, \quad \frac{\partial \hat{\boldsymbol{k}}}{\partial \hat{C}} = \begin{bmatrix} 1 \\ 0 \\ 0 \end{bmatrix}, \quad \frac{\partial^2 \hat{\boldsymbol{k}}}{\partial \hat{C}^2} = \begin{bmatrix} 0 \\ 0 \\ 0 \end{bmatrix}, \quad \frac{\partial^2 \hat{\boldsymbol{k}}}{\partial \theta^2} = \hat{D}_{12} \begin{bmatrix} -2 \\ 2 \\ 0 \end{bmatrix}, \quad \frac{\partial^2 \hat{\boldsymbol{k}}}{\partial \hat{C}\, \partial \theta} = \begin{bmatrix} 0 \\ 0 \\ 2 \end{bmatrix}.$$

At the second equilibrium position, $\partial^2 \hat{U} / \partial \hat{C}^2 = 1$ and $\partial^2 \hat{U} / \partial \theta\, \partial \hat{C} = 0$. Thus, the existence of a minimum, and hence stability, depends on the sign of $\partial^2 \hat{U} / \partial \theta^2$. The system will be stable for

$$\frac{\partial^2 \hat{U}}{\partial \theta^2} > 0,$$

and so, substituting into (4.8) the terms that correspond to the second equilibrium configuration, computed above, gives

$$(\hat{D}_{12})^2 \left(4\hat{D}_{66} + 2\hat{D}_{12} - 2\frac{\hat{D}_{22}}{\hat{D}_{12}} \right) > 0. \tag{5.1}$$

Thus, the existence of a second stable equilibrium depends entirely on the sign of the second bracketed term in (5.1). In other words, defining

$$S = 4\hat{D}_{66} + 2\hat{D}_{12} - 2\frac{\hat{D}_{22}}{\hat{D}_{12}}, \tag{5.2}$$

the structure is bistable for $S>0$.

It is interesting to study (5.2) to see the effects that individual components of the $\boldsymbol{D}$-matrix have on the existence of a second stable solution. Increasing the twisting stiffness (D_{66}), and increasing the coupling between bending in the x- and y-directions (D_{12}) will tend to make a shell bistable. Decreasing the bending stiffness in either the x-direction (D_{11}), or the y-direction (D_{22}) will also tend to make a shell bistable (because decreasing D_{11} will *increase* $\hat{D}_{66}$ and $\hat{D}_{12}$).

6. Relaxing the inextensional constraint

For shells that have a non-zero $\boldsymbol{B}$ matrix, i.e. where there is coupling between stretching and bending deformations, the assumption that the in-plane strains are zero is unnecessarily restrictive. In this case, even when the shell is thin, in-plane strains will occur a natural consequence of bending deformation.

Without changing the fundamental assumption of the inextensional model, a minor amendment of the $\boldsymbol{D}$ matrix allow uniform in-plane strains to be included in the formulation.

Starting from (2.1) we write, in compact form

$$\begin{bmatrix} \boldsymbol{A} & \boldsymbol{B} \\ \boldsymbol{B}^{\mathrm{T}} & \boldsymbol{D} \end{bmatrix} \begin{bmatrix} \boldsymbol{\epsilon} \\ \boldsymbol{k} \end{bmatrix} = \begin{bmatrix} \boldsymbol{f} \\ \boldsymbol{m} \end{bmatrix}. \tag{6.1}$$

If we assume $\boldsymbol{f}=\boldsymbol{0}$, instead of $\boldsymbol{\epsilon}=\boldsymbol{0}$ as in the earlier formulation, we find that (3.3) is replaced by

$$(\boldsymbol{D}-\boldsymbol{B}^{\mathrm{T}}\boldsymbol{A}^{-1}\boldsymbol{B})\boldsymbol{k} = \boldsymbol{m}, \tag{6.2}$$

and introducing the 'reduced' bending stiffness $\boldsymbol{D}^{*}$

$$\boldsymbol{D}^{*} = \boldsymbol{D}-\boldsymbol{B}^{\mathrm{T}}\boldsymbol{A}^{-1}\boldsymbol{B}, \tag{6.3}$$

the rest of the analysis is then unchanged. For practical shells, $\boldsymbol{D}^{*}$ is not very different from $\boldsymbol{D}$, and indeed when $\boldsymbol{B}=\boldsymbol{0}$ they are identical.

7. Discussion

The results in §4 are in qualitative agreement with observations from simple models. Isotropic shells are not bistable; simple antisymmetric layups of composites are bistable. Symmetric layups of composites tend to coil into a helix rather than a compact coiled state.

The results in this paper are also in very good quantitative agreement with the results of various more complex analytical and computational models presented in Iqbal & Pellegrino (2000) and Galletly & Guest (2004*a*,*b*). In particular, the

results are identical to the analytical results in Galletly & Guest (2004*a*,*b*) for the cases when β, the angle that the shell subtends in the initial state, is large.

Previously, Hyer and co-workers (e.g. Hyer 1981; Dano & Hyer 1998) have studied a closely related problem, the non-planar room-temperature shape of non-symmetric composites that were initially laid-up flat. They assumed a simple out-of-plane displacement field, but adopt a second-order strain formulation to capture the out-of-plane instability of these plates. By contrast, the inextensional model presented here works in terms of *curvatures*, which allow us to adopt a linear kinematic model, giving a much simpler, although less general, formulation.

All of the work in this paper has assumed that the shells are stress-free in their initial configuration; however, isotropic shells can also be made bistable by an initial state of self-stress. Kebadze *et al.* (2004) develops the inextensional model presented in this paper to deal with these cases.

8. Conclusion

The equilibrium configurations of a cylindrical shell can be determined by solving (4.4) and the stability of each configuration can then be tested by checking the positive definiteness of (4.5). If bending and twisting are decoupled in the $\boldsymbol{D}$ matrix, then the test for positive definiteness reduces to (5.2).

We would like to thank Buba Kebadze, Khuram Iqbal and Diana Galletly for helpful discussions, and Shamala Sambasivam for making the model shown in figure 1. The work was partially funded by the EPSRC. Simon Guest acknowledges support from the Leverhulme Trust, and Harvard University Division of Engineering and Applied Sciences.

References

Calladine, C. R. 1983 *Theory of shell structures*. Cambridge, UK: Cambridge University Press.

Dano, M. L. & Hyer, M. W. 1998 Thermally-induced deformation behavior of unsymmetric laminates. *Int. J. Solids Struct.* **35**, 2101–2120. (doi:10.1016/S0020-7683(97)00167-4)

Galletly, D. A. & Guest, S. D. 2004*a* Bistable composite slit tubes I: a beam model. *Int. J. Solids Struct.* **41**, 4517–4533. (doi:10.1016/j.ijsolstr.2004.02.036)

Galletly, D. A. & Guest, S. D. 2004*b* Bistable composite slit tubes II: a shell model. *Int. J. Solids Struct.* **41**, 4503–4516. (doi:10.1016/j.ijsolstr.2004.02.037)

Hyer, M. W. 1981 Calculation of the room-temperature shapes of unsymmetric laminates. *J. Compos. Mater.* **15**, 296–310.

Iqbal, K. & Pellegrino, S. 2000 Bi-stable composite shells. *Proc. 41st AIAA/ASME/ASCE/AHS/ASC Structures, Structural Dynamics, and Materials Conference and Exhibit, 3–6 April 2000, Atlanta, GA, USA.*

Iqbal, K., Pellegrino, S. & Daton-Lovett, A. 2000 Bi-stable composite slit tubes. In *Proc. IUTAM-IASS Symposium on Deployable Structures, 6–9 September 1998* (ed. S. Pellegrino & S. D. Guest), pp. 153–162. Cambridge, UK: Kluwer.

Jones, R. M. 1999 *Mechanics of composite materials*, 2nd edn. Philadelphia, PA: Taylor & Francis.

Kebadze, E., Guest, S. D. & Pellegrino, S. 2004 Bistable prestressed shell structures. *Int. J. Solids Struct.* **41**, 2801–2820. (doi:10.1016/j.ijsolstr.2004.01.028)

Mansfield, E. H. 1989 *The bending and stretching of plates*, 2nd edn. Cambridge, UK: Cambridge University Press.

Riley, K. F., Hobson, M. P. & Bence, S. J. 1997 *Mathematical methods for physics and engineering*. Cambridge, UK: Cambridge University Press.